A DIFFUSE SOFT X-RAY SPECTROMETER

Dan McCammon

Department of Physics, University of Wisconsin, Madison

Abstract

A design for a diffuse X-ray spectrometer utilizing Bragg reflection is described. The geometry has a very high throughput for a given physical size and allows simultaneous observation at all wavelengths within its range. An implementation with overall dimensions about 33 x 66 x 66 cm uses 1800 cm^2 of lead stearate multilayer Bragg reflector to cover the wavelength range 42 to 84 Angstroms with a throughput of about 0.01 cm^2 sr, including detector efficiency. Spectral resolving power is about 35 to 50. A similar unit equipped with thallium acid pthallate crystals will cover the 11 - 24 A range with about half this throughput and twice the resolving power.

I. INTRODUCTION

There is now strong evidence indicating that most of the diffuse X-ray background at energies less than 1 keV is local to the Galaxy (Sanders et al. 1977). Discrete sources seem to account for at most a small fraction of this, at least below 0.3 keV (Vanderhill et al. 1975; Rosner et al. 1981). The lack of acceptable non-thermal diffuse emission mechanisms (Williamson et al. 1974) leads to the conclusion that most of this X-ray flux is due to thermal emission from a hot ($T \sim 10^6$ K), tenuous component of the interstellar medium. It has been argued on theoretical grounds that such material occupies a large fraction of the volume of the Galactic disk, with a filling factor perhaps as high as 0.5 - 0.9 (Cox and Smith 1974; Smith 1977; McKee and Ostriker 1977). If this is true (and the ubiquity of O VI absorption in the ultraviolet lends considerable credence to the idea: see review by Jenkins 1977), then the hot component must have a profound influence on the nature of the ISM, and any comprehensive understanding of Galactic structure and evolution will require much more detailed knowledge of this high temperature material than we currently possess (McCray and Snow 1979, and references therein).

Our picture of the ISM is getting so complicated that broad-band spectral measurements are no longer adequate for testing the more detailed and complex models now being proposed. Fortunately, radiation from gas around 10^6 K with any reasonable composition is almost entirely in characteristic lines of the heavier elements, and observations of these can in principle supply a wealth of information on physical conditions within this component, and even its past history. Interpretation

of spectra will admittedly be complicated considerably by multiple temperatures, abundance variations, and non-equilibrium conditions, but optical spectroscopy has had to deal with similar or even more severe complications and still managed to make significant contributions to astrophysical understanding.

II. OBSERVATIONAL APPROACHES

The following are possible avenues to observing interstellar gas at $\sim 10^6$ K:

1. Optical and U.V. forbidden lines: These have been observed in some high surface brightness supernova remnants, but seem hopelessly faint from the general ISM.
2. Resonance absorption lines: In this temperature range, only the O VI lines fall longward of the Lyman limit. The anomalously low local neutral hydrogen density might allow observation of other lines in the XUV out to a distance of 100 pc or so, and could provide much useful information about the solar neighborhood. Observation of absorption lines in the X-ray region could be done against bright Galactic X-ray sources with AXAF-class instrumentation and should give some very interesting results. However, suitable sources are few in number and almost all at large distances, so only a very limited amount of information can be obtained in this way.
3. Photoionization signatures: One could conceivably look for evidence of absorption of X-ray and XUV photons in surrounding cooler material. However, none of the accessible resulting states seems sufficiently unique to make this a practical approach.

4. X-ray emission lines: These represent the dominant cooling mechanism for the hot gas and have potentially the highest information content. One of the major observational difficulties is the low surface brightness. Since this is a true diffuse source, collecting or focussing optics can serve only to increase spatial resolution, which will be desirable someday, but in a first-generation instrument the additional inefficiency introduced by these elements would exacerbate the major problem of getting enough photons.

III. TYPES OF SPECTROSCOPIC INSTRUMENTS

Possible instrumental types for moderate-resolution spectroscopy below 1 keV include:

1. Solid state detectors: These have wide acceptance angles, but at the current state of the art give little improvement over proportional counters below 1 keV.

2. Reflection gratings: Allow observation of all wavelengths simultaneously, but must be used near grazing incidence, making acceptance angles and throughput extremely small for diffuse sources.

3. Transmission gratings: Small dispersions again require small acceptance angles. Efficiency is also lower than reflection gratings.

4. Bragg crystals and multi-layer analyzers: These have relatively high integrated reflectivities, can work at large angles, and thus can have relatively high throughput. Their major disadvantage is that a given crystal area can be used for only one wavelength at a time, if all incoming X-rays are arriving from the same direction.

For studying the diffuse background, we can get around the problem of one wavelength at a time when using Bragg reflection by looking at many wavelengths simultaneously, but from different parts of the sky. The spatial coverage can either be smeared out to get an average spectrum or sorted out by spatial bins as the instrument pointing is changed to eventually obtain a complete spectrum of each spatial element while retaining the spectral multiplex advantage. The following section describes one geometry which has been worked out to take advantage of this scheme.

IV. GEOMETRY FOR A DIFFUSE X-RAY BRAGG SPECTROMETER

To obtain a finite counting rate from a truly diffuse source, the detector must accept X-rays from a finite range of angles. To keep the Bragg reflection angle (and thus the observed wavelength) from changing as fast as the angle with respect to the detector, the crystal can be curved to compensate for the changing look direction, keeping the reflection angle constant. For a one-dimensional detector, the required curve is an exponential spiral. This allows the field of view to be made as large as desired without affecting the spectral resolution, but it works only for a single wavelength.

Our approach is to extend a position-sensitive detector along the x-axis, and to make the curvature of the crystal above each point on the counter appropriate to an exponential spiral about that point, subject to the constraints that the crystal be continuous and have a continuous slope. This allows the use of a plane detector with a simply constructed collimator directed perpendicular to the counter face at all

positions. The reflection angle for rays perpendicular to the detector will vary with position on the x-axis, but at any given position there will be no change in this angle to first order as the collimation angle departs from perpendicular. The shape thus determined for the crystal turns out to be a circular cylinder, with the detector located along a diameter, as shown in Figure 1. This makes it simple to calculate analytic expressions for parameters of interest, which are given in Table 1. These follow from the Bragg condition, $\lambda = 2d \sin \theta'$, the exact expression $\cos \theta' = \cos \theta \cos \Delta\phi$, and the approximation $\sin \theta' \approx \sin \theta \cos \Delta\psi$, where θ is the reflection angle for the ray perpendicular to the detector, and θ' is the reflection angle for a ray which is at an angle $\Delta\phi$ from perpendicular in the dispersion direction or $\Delta\psi$ from perpendicular in the cross direction. As can be seen from these expressions, going off-axis in the dispersion direction always increases the wavelength from the nominal value at that x-position, while going off-axis in the cross direction always decreases it. These effects partially cancel over most of the off-axis field of view, and the FWHM of the resulting profile is less than half the $\Delta\lambda$ calculated using the FWHM angle of the collimator.

Figure 2 shows a cross section of an instrument as it might be built using a lead stearate (PbSt) Bragg reflector to cover the 148-295 eV band. The inherent resolving power of PbSt varies from 40 to 60 over this range and the collimation angles on the detector can be opened up to 20° x 20° FWHM before this is degraded by a factor of $\sim \sqrt{2}$. A ray-tracing computer model has been written to predict the response of such an instrument to an arbitrary input spectrum. The program takes into account off-axis

rays, vignetting, collimator transmission, and detector efficiency for a practical proportional counter, as well as the full rocking curve and specular reflection of the Bragg crystals. The latter were measured for PbSt at the Tantalus synchrotron radiation facility of the University of Wisconsin's Physical Sciences Laboratory, using a grating double monochrometer. The high intensity, low scattered light, and steep-skirted 0.5 A bandpass of this source allowed measurements of the wings of the rocking curve down to three orders of magnitude below the peak, and specular reflectivity out to angles where it dropped below 10^{-5}. These parameters are important in determining the response of a Bragg spectrometer to such quasi-continuous sources as astrophysical plasmas.

Calculations for the geometry of Figure 2 with a detector 23 cm wide in the x-direction and both detector and crystal 53 cm long give a throughput as shown in Figure 3. Figure 4 shows the calculated response to a sky uniformly bright in boron and carbon K-alpha emission. The natural widths of these lines when they are excited from elemental solids as published by Holliday (1967) have been included; the response to a monochromatic line of the same nominal wavelength is shown by the dashed line. A spectrometer has been built to the above specifications and exposed to large alpha-particle excited targets of boron and carbon which entirely filled its field of view. The data points in Figure 4 show its response. (The horizontal scale, for which nominal wavelengths are given, is linear in x-position on the detector. The position resolution of the proportion counter is about 1 mm FWHM at 70 eV pulse height, and does not contribute significantly to the line profile widths.) We do not know why

the boron line appears significantly narrower than the published profile, but this has also been noticed when testing flat crystal samples in a monochrometer with an electron-excited boron source. The spreading of the profiles at low amplitudes (most noticeable on the long-wavelength wing of the carbon line) is probably due to imperfections in the cylindrical figure at the edges of the individual elements of the mosaic crystal panel. Absolute intensity calibrations of the sources agree with the calculated throughput to better than 15% for both lines.

Figure 5a shows the response to a two-temperature Raymond and Smith (1977) thermal spectrum which has been fit to three-band sky survey data for a typical region in the southern hemisphere. The brighter lines in the spectrum are also indicated as they appear before being folded through the instrumental response. The dashed line shows the contribution due to the cosmic-ray background level predicted by laboratory measurements (6×10^{-4} counts cm^{-2} s^{-1} keV^{-1}). It slopes because the pulse height limits used in integrating the signal have been varied with position on the counter to roughly optimize the signal to noise ratio. Figure 5b shows the same response integrated into position bins for an assumed 5000-second observation, with the resulting number of counts in each bin further subjected to a Poisson randomization. For this and the following figures showing the PbSt bandpass, the collimation angles have been reduced to 10° x 10° FWHM in order to preserve essentially the full inherent resolving power of the crystals.

A similar geometry can be used with other Bragg crystals. Thallium acid pthallate (TAP) shows the greatest promise for covering the interesting

M band region (.5 - 1.0 keV) where the number of important lines is not so large as at lower energies and the physics should be easier to disentangle. Unfortunately, the much higher inherent resolving power of TAP means that the integrated reflectivity is lower than for PbSt, and this, coupled with the much lower fluxes, means that long observing times will be necessary. Figure 6 shows the predicted results from an instrument the same size as the PbSt spectrometer, but using a TAP crystal to cover the 516 to 1032 eV range. The collimation angle has been opened up to 15° x 15° in order to increase the throughput, and as a result the observed line profile widths are almost entirely due to effects of the collimation angles. Even thermal equilibrium fits to the three-band sky survey data are not unique, and Figures 7 and 8 show the result of two different multicomponent spectral fits to another part of the sky. These are one- and three-temperature fits with equilibrium models, and while non-equilibrium models would certainly be different, they are unlikely to be significantly more complex.

V. OTHER BRAGG REFLECTORS

No natural crystals have 2d spacings long enough to cover the 150-300 eV region, and PbSt is the best material tested so far for a Langmuir-Blodgett multilayer analyzer. For the 500-1000 eV range, TAP has the highest integrated reflectivity of commercially available crystals.

However, recent successful work with artificial multilayers is very promising (Spiller et al. 1980; Barbee 1981; Underwood and Barbee 1981). The rocking-curve width of PbSt is actually rather well matched to the

resolving power which could be used on even a fairly lengthy shuttle-based observation. The materials are also nearly optimum and there is probably not more than a factor of two to be gained by going to an optimized artificial multilayer. TAP, on the other hand, has an inherent resolving power of about 10^3, which is much higher than can be used with expected observing times and instrumental backgrounds, and we calculate a factor of five potential improvement for artificial multilayers that seem feasible to fabricate.

VI. CONCLUSIONS

Spectroscopy of the Galactic component of the diffuse X-ray background is necessary for an adequate understanding of the coronal phase of the interstellar medium. This is especially important if this phase is as pervasive as has been predicted.

Whether this spectroscopy eventually is done with an instrument similar to the one described here, or with some more clever specialized design, or as a sideline by a much larger general-purpose instrument, two major characteristics must be kept in mind and designed in. The first of these is simply high throughput. It is probably impractical to attempt these observations with less than about 10% of the area-solid angle factor of the examples in this paper. For an imaging telescope with a small field of view, this implies very large areas. For example, an imaging instrument equipped with very high efficiency (50%) objective reflection gratings and having about the same physical size as the two instruments described above put together has about three orders of magnitude less throughput.

The second vital consideration is a low-background detector. The Bragg spectrometers whose responses are shown in Figures 5-8 have about aslarge a convergence angle at the detector and as high an optical efficiency as is practical to design into an instrument, particularly a general-purpose imager, and so we expect that these simulations represent an upper limit to the surface brightness of the spectrum at the detector. Even so, it can be seen that they are very nearly cosmic-ray background limited at an assumed background rate of 6×10^{-4} counts cm^{-2} s^{-1} keV^{-1} between 70 eV and 1000 eV. During a sounding-rocket flight, position-sensitive proportional counters showed a cosmic-ray background rate (door-closed or earth-looking) which was actually about one-third of this, but with the spectrometer field-of-view exposed to the sky an additional background due to electrons scattering off the crystal panel and penetrating the counter windows was observed. This can be reduced adequately with magnetic field screens, but there is also another sky-related background which may be due to a softer and much more intense component of the electron flux producing fluorescence and bremmsstrahlung X-rays as they strike the crystal panel.

This is brought up to emphasize the care that must be taken to minimize all extraneous sources of background at the detector, whether from cosmic rays, scattered electrons, or stray ultraviolet, if there is any intention of making these interesting and potentially important measurements.

TABLE 1. GEOMETRICAL CHARACTERISTICS

$$\lambda = 2d \sin \Theta = 2d \frac{y}{R} = 2d \sqrt{1-\left(\frac{x}{R}\right)^2}$$

x = distance from center of curvature, O.

If: I_λ = source brightness in photons cm^{-2} s^{-1} $sterad^{-1}$

and: $(A^*\Omega)_\lambda$ = spectrometer throughput in cm^2 sterad

Then counting rate = $I_\lambda (A^*\Omega)_\lambda$.

$$(A^*\Omega)_\lambda = \ell R \, R_I(\lambda) \Delta\phi \, \Delta\psi \sin \Theta_B(\lambda) \, \varepsilon_\lambda.$$

Where: ℓ = length of detector and crystal

R = crystal radius of curvature

$R_I(\lambda)$ = integrated reflectivity of crystal

$\Delta\phi$ = collimation HWB in dispersion direction

$\Delta\psi$ = collimation HWB in cross direction

$\Theta(\lambda)$ = Bragg angle

ε_λ = detector efficiency

Contributions to limited resolving power:

A) Collimation in dispersion direction:

$$\frac{\lambda}{\Delta\lambda} \approx \frac{-2 \tan^2 \Theta}{\Delta\phi^2}$$

B) Collimation in cross-dispersion direction:

$$\frac{\lambda}{\Delta\lambda} \approx \frac{2}{\Delta\psi^2}$$

C) Position resolution of detector:

$$\frac{\lambda}{\Delta\lambda} = \sin \Theta \tan \Theta \frac{R}{\Delta x}$$

D) Finite width of crystal Rocking curve:

$$\frac{\lambda}{\Delta\lambda} = \tan \Theta \frac{1}{\Delta\Theta}$$

REFERENCES

Barbee, Troy W. Jr. 1981, Proceedings of the Topical Conference on Low-Energy X-ray Diagnostics, A.I.P., Monterey, Calif. (Preprint).

Cox, D. P., and Smith, B. W. 1974, Ap. J., 189, L105.

Holliday, J. E. 1967, Norelco Reporter, XIV, 84.

Jenkins, E. B. 1977, in Topics in Interstellar Matter, H. van Woerden ed., Dordrecht, Reidel.

McCray, R., and Snow, T. P. Jr. 1979, Ann. Rev. Ast. and Ap., 17, 213.

McKee, C. F., and Ostriker, J. P. 1977, Ap. J., 218, 148.

Raymond, J. C., and Smith, B. W. 1977, Ap.J.(Suppl.), 35, 419.

Rosner, R., Avni, Y., Bookbinder, J., Giacconi, R., Golub, L., Harnden, F. R. Jr., Maxson, C. W., Topka, K., and Vaiana, G. S. 1981, preprint (to be published in Ap.J. (Letters)).

Sanders, W. T., Kraushaar, W. L., Nousek, J. A., and Fried, P. M. 1977, Ap.J., 217, L87.

Smith, B. W. 1977, Ap.J., 211, 404.

Spiller, Eberhard, and Segmüller, Armin 1980, Appl. Phys. Lett., 37, 1048.

Underwood, J. H., and Barbee, T. W. Jr. 1981, Proceedings of the Topical Conference on Low-Energy X-ray Diagnostics, A.I.P., Monterey, Calif. (Preprint).

Vanderhill, M. J., Borken, R. J., Bunner, A. N., Burstein, P. H., and Kraushaar, W. L. 1975, Ap.J. (Letters), 197, L19.

Williamson, F. O., Sanders, W. T., Kraushaar, W. L., McCammon, D., Borken, R., and Bunner, A. N. 1974, Ap.J., 193, L133.

FIGURE CAPTIONS

Figure 1: The Bragg reflector is on the inner surface of the circular cylinder of radius R. The detector occupies a portion of the x-axis below the reflector.

Figure 2: Cross section of an instrument to cover the energy range 148-195 eV, showing sample ray tracings.

Figure 3: Area-Solid Angle product vs. photon energy for a PbSt spectrometer with a 23 cm x 53 cm proportional counter detector and 20° x 20° collimation.

Figure 4: Predicted and actual responses of a PbSt spectrometer with 20° x 20° collimation to uniform diffuse illumination of the field of view with boron and carbon K-alpha radiation. The dashed curve shows the predicted response to a monochromatic line of the same nominal wavelength.

Figure 5a: Predicted response of a PbSt spectrometer with 10° x 10° collimation to a two-temperature equilibrium plasma model fit to observed broad-band counting rates at a typical region in the southern Galactic hemisphere. The brighter lines also are shown before folding through the spectrometer response. The right-hand scale gives the individual line intensities, the left-hand scale gives spectrum surface brightness on the detector.

FIGURE CAPTIONS, cont.

b: The above spectrum integrated into bins over an assumed 5000-second observation, with the counts in each bin subsequently modified by a Poisson-distributed Monte-Carlo procedure.

Figure 6a: The spectrum of figure 5 folded through a TAP spectrometer with 15° x 15° collimation which covers the 515 - 1030 eV range.

b: The above spectrum integrated for 5000 seconds, binned and randomized.

Figure 7a: PbSt spectrum of three-temperature fit to a part of the North Polar Spur.

b: TAP response to above spectrum.

Figure 8a: Single temperature plus power law fit suggested by Nagoya Univ. group for data from North Polar Spur. PbSt spectrometer.

b: As above, but TAP spectrometer response.

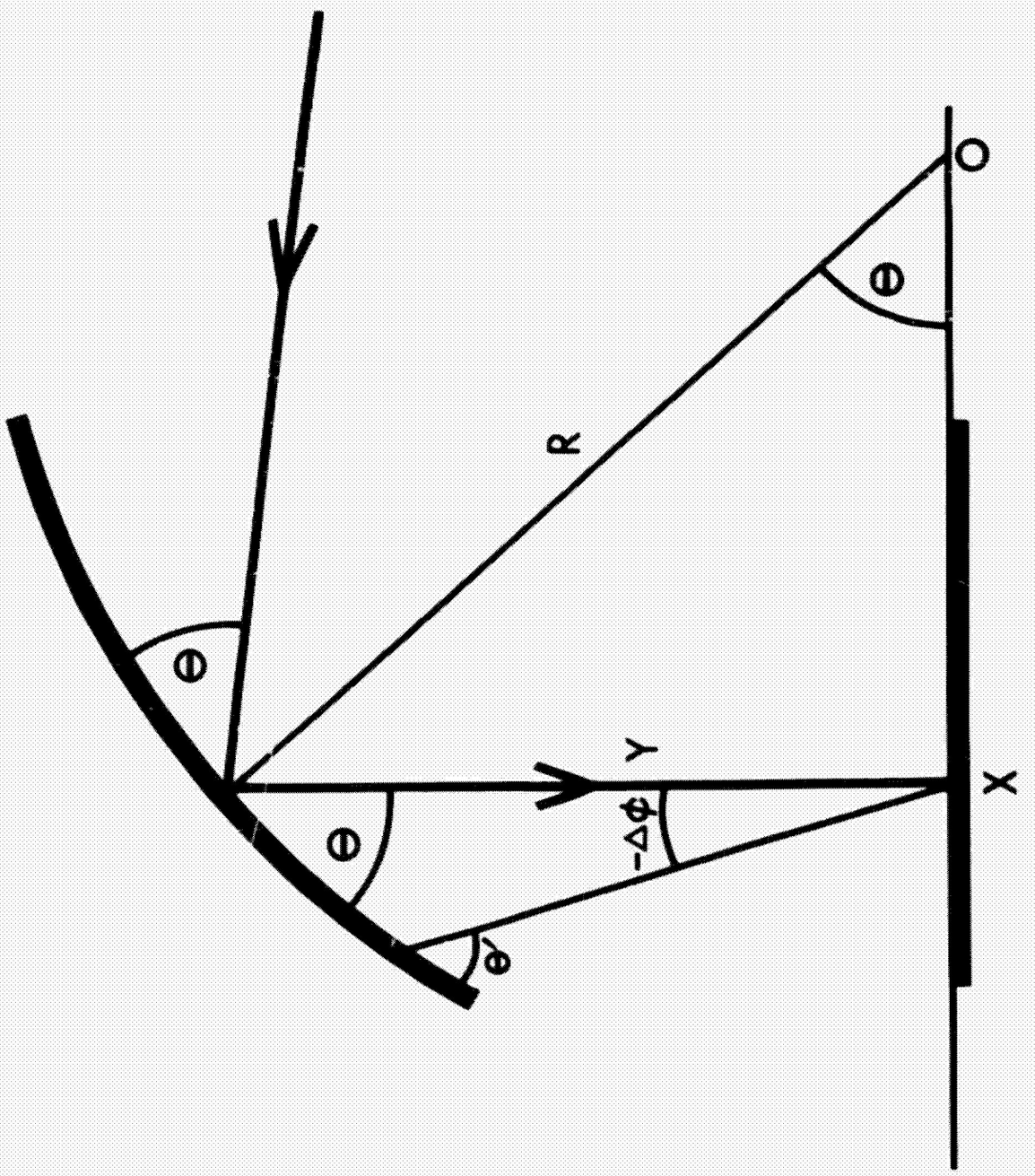

FIGURE 1

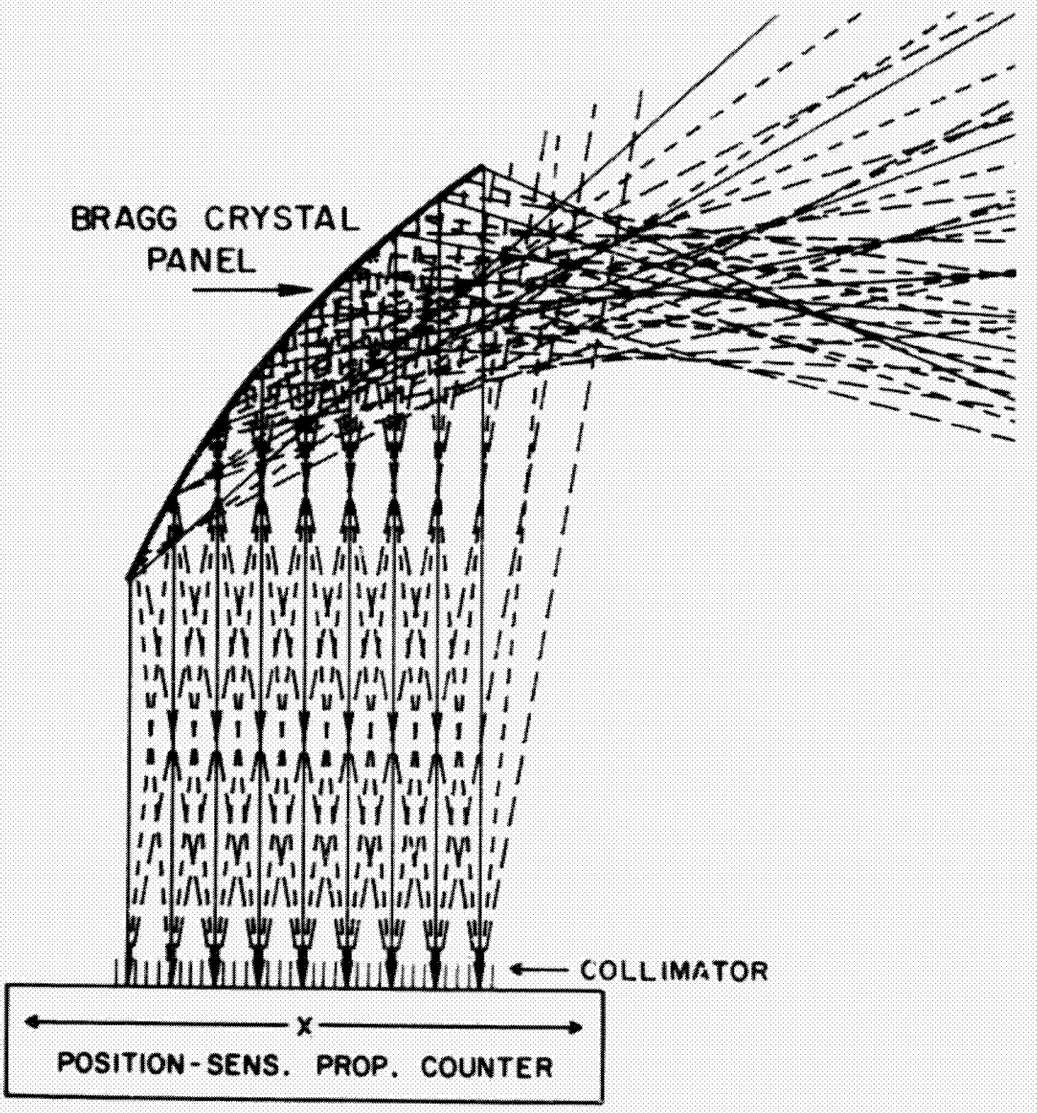

FIGURE 2

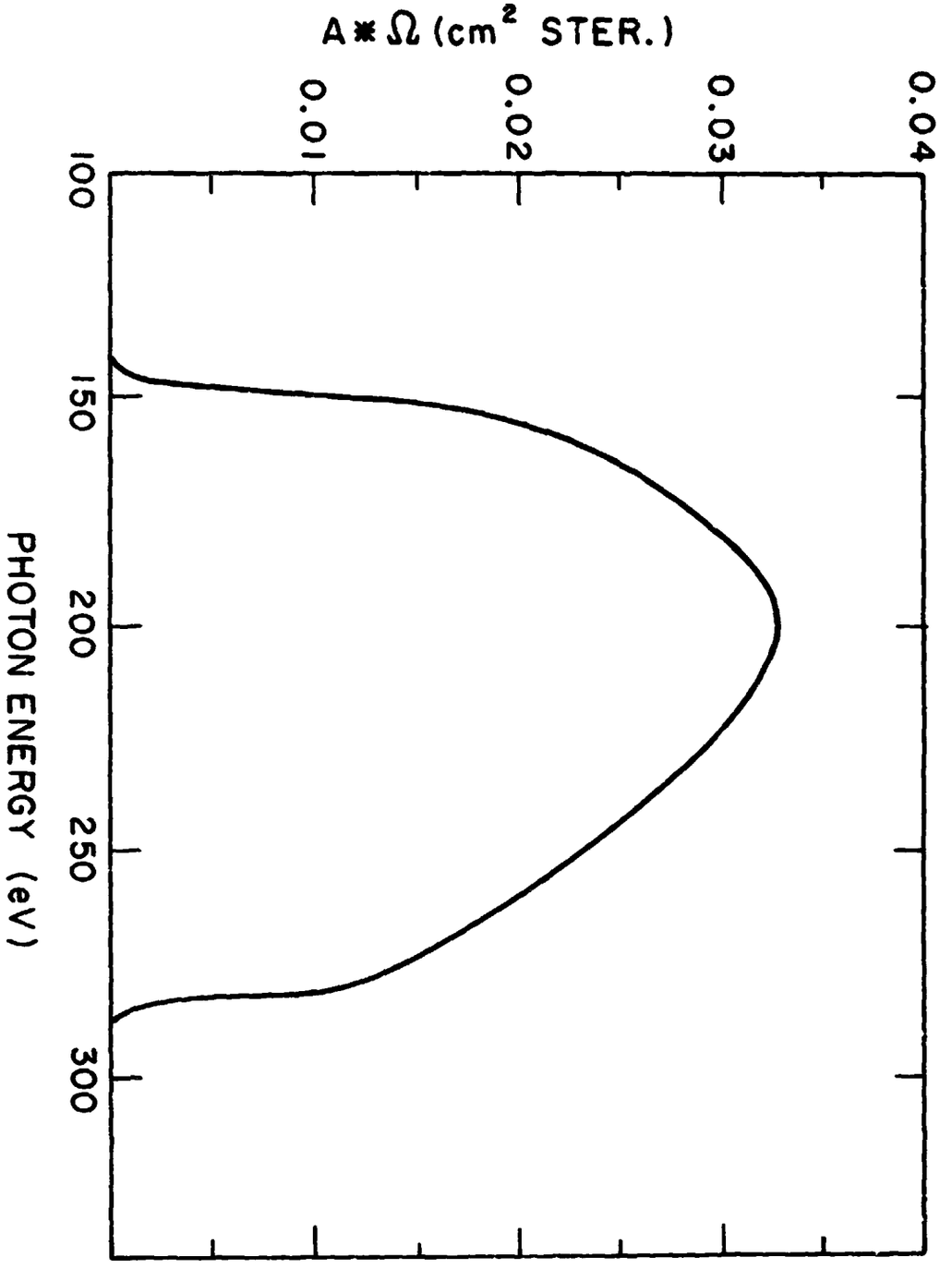

FIGURE 3

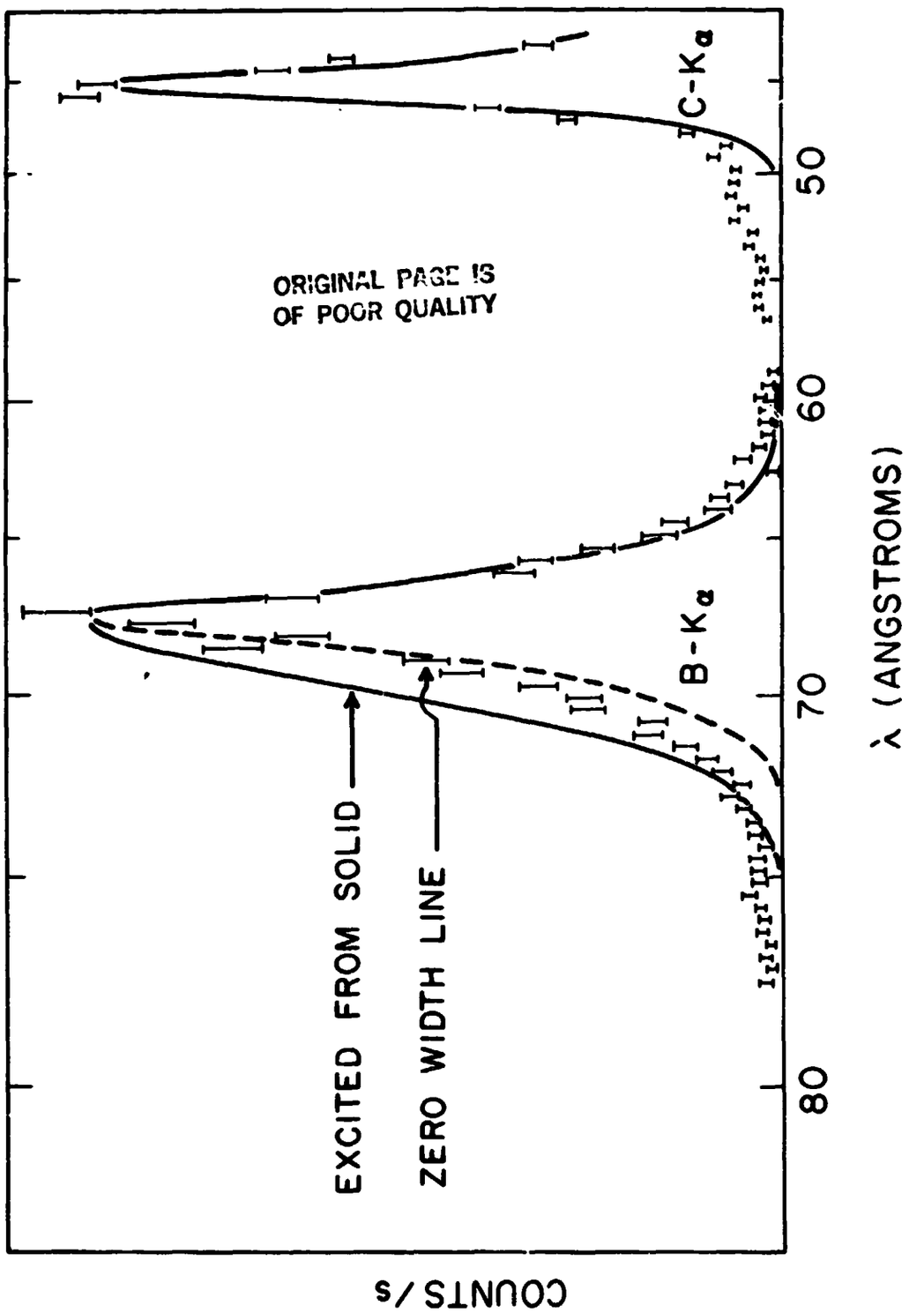

FIGURE 4

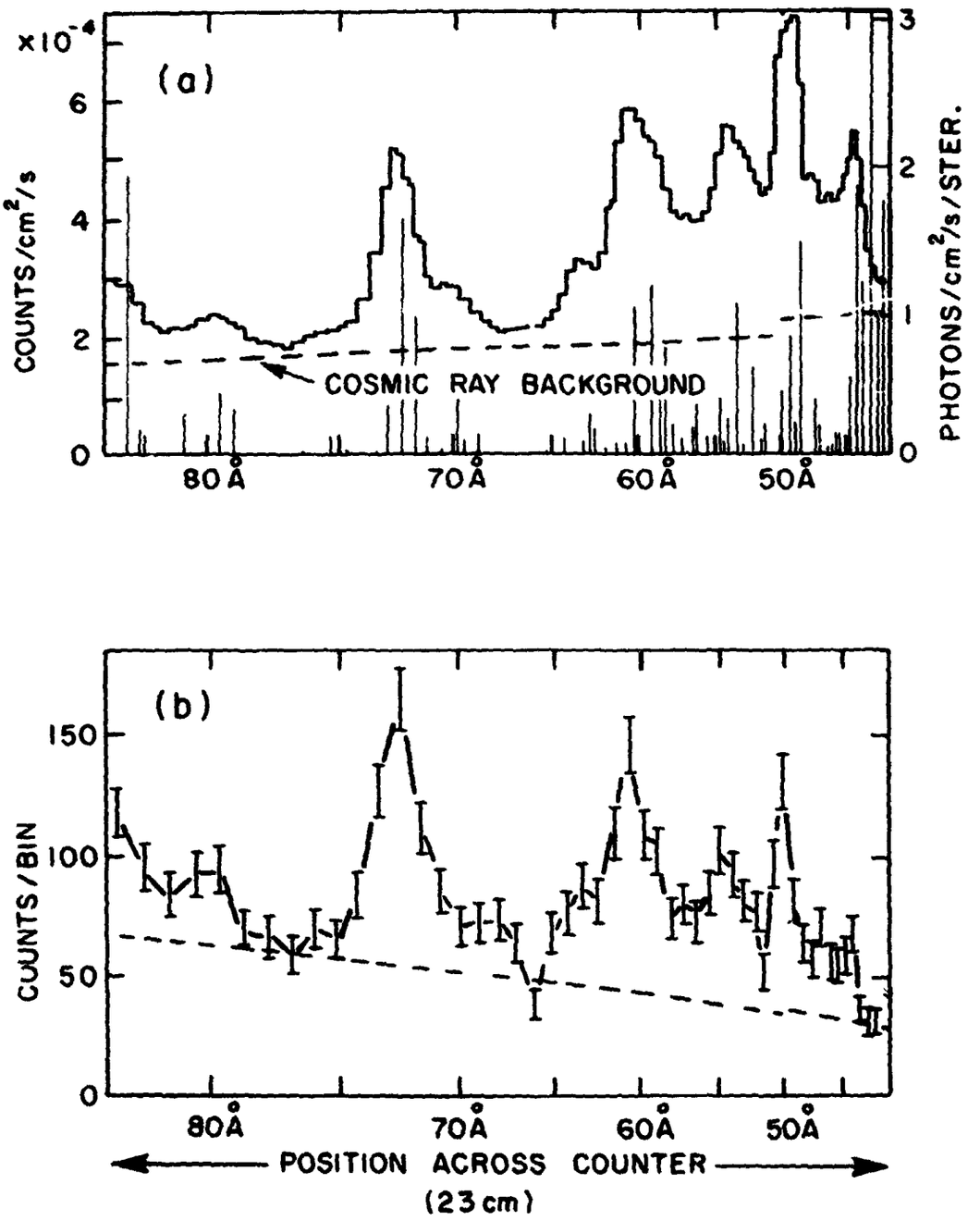

FIGURE 5

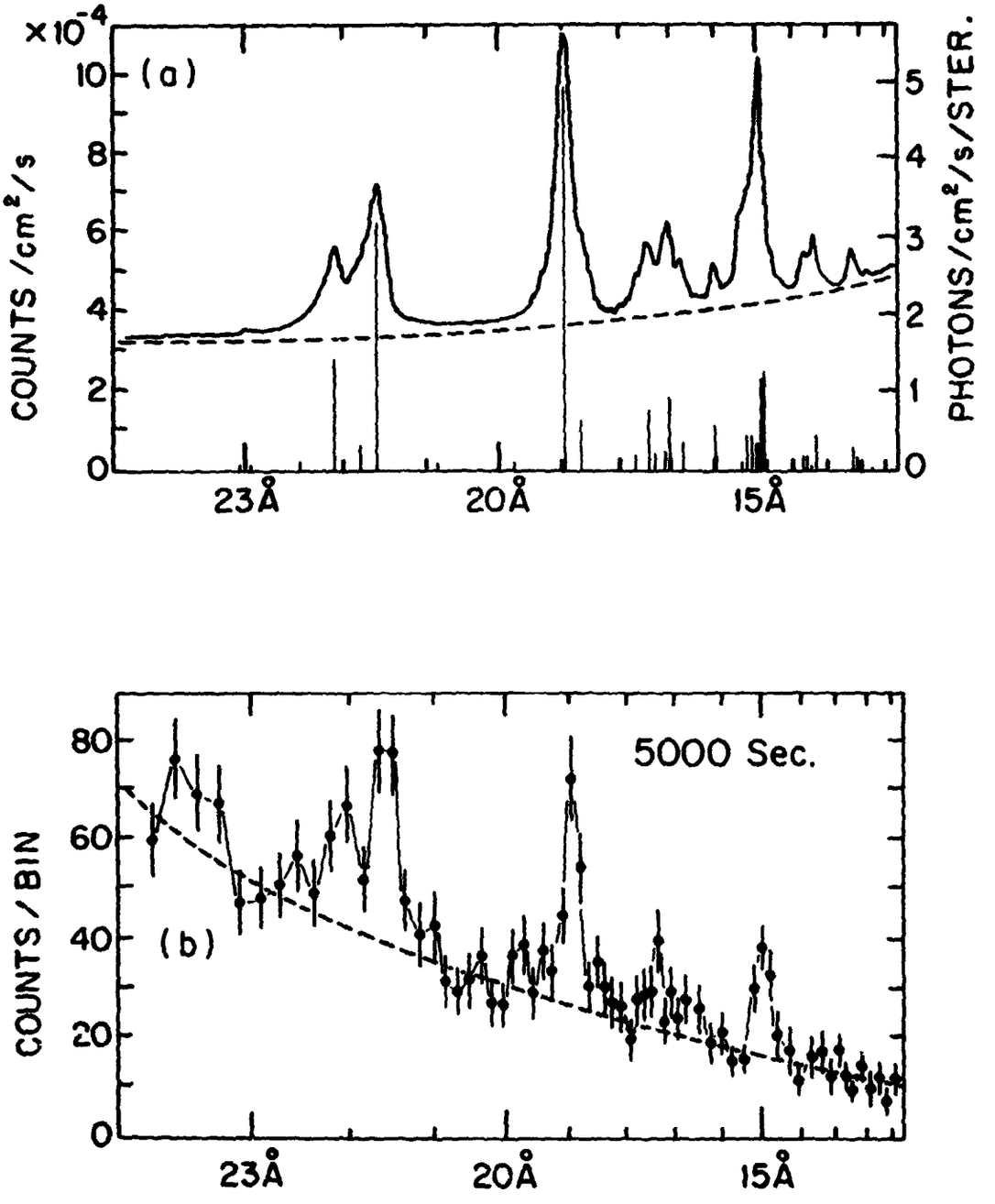

FIGURE 6

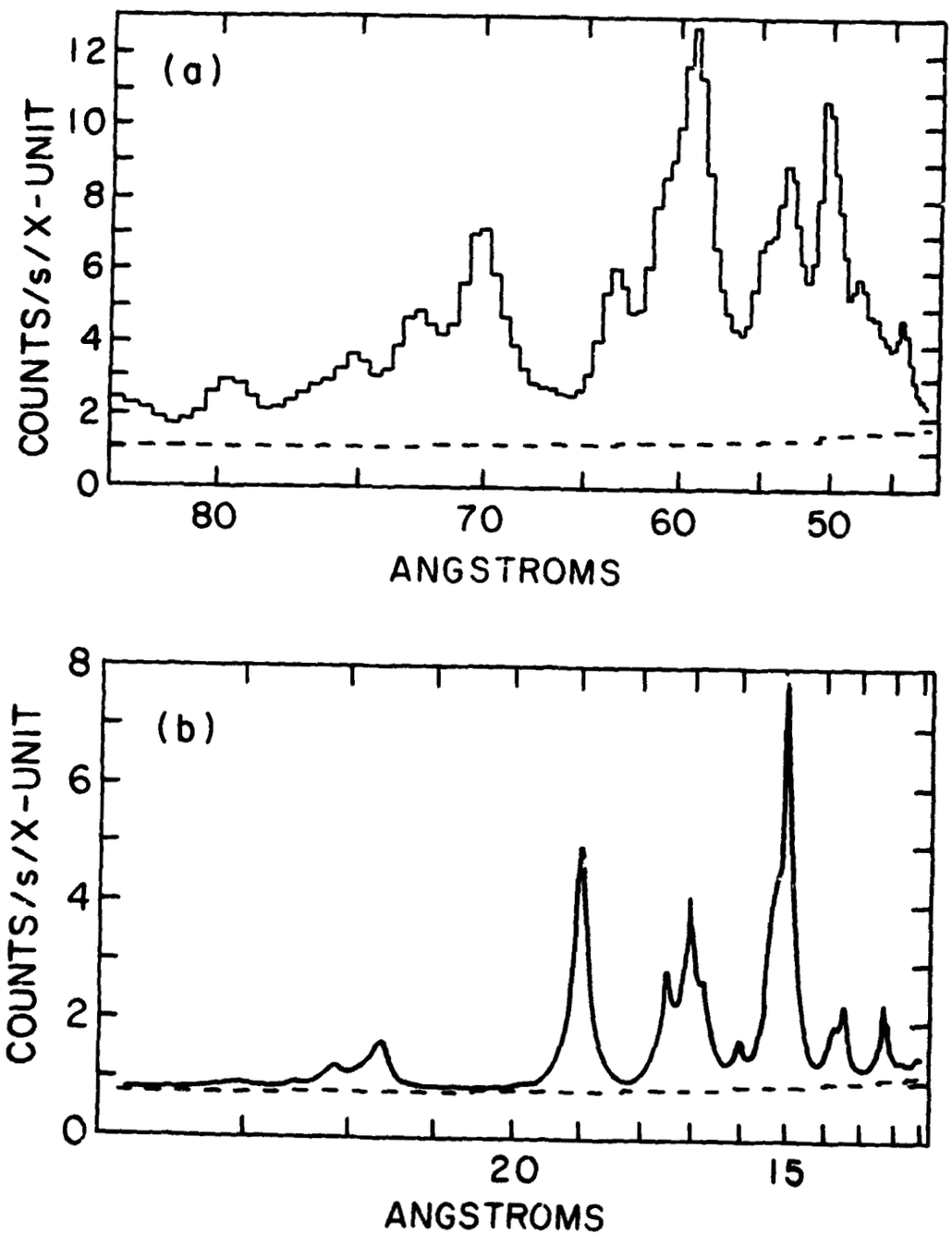

FIGURE 7

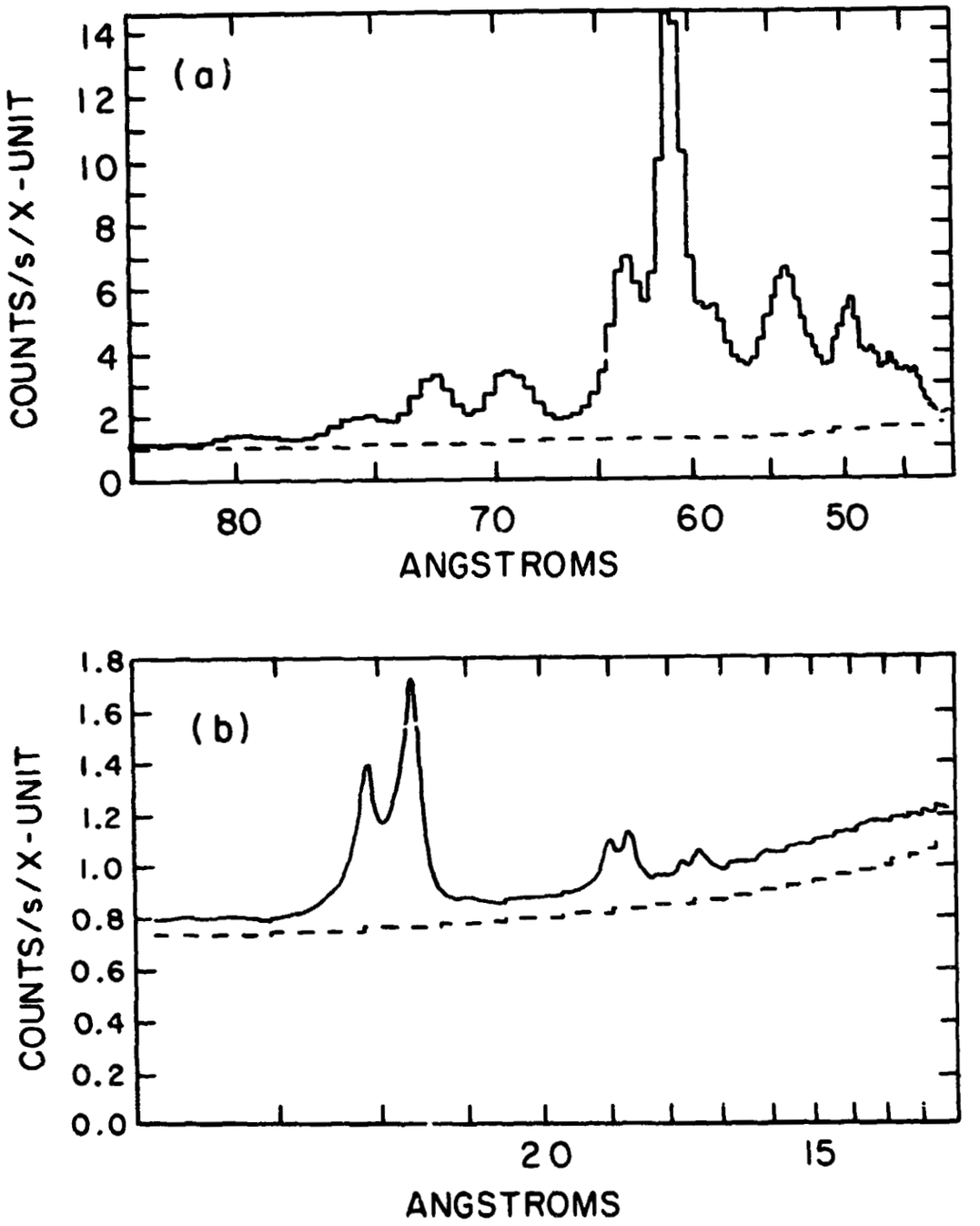

FIGURE 8